

Validation of the Glaucoma Filtration Surgical Mouse Model for Antifibrotic Drug Evaluation

Li-Fong Seet,¹ Wing Sum Lee,¹ Roseline Su,¹ Sharon N Finger,¹ Jonathan G Crowston,² and Tina T Wong^{1,3,4,5}

¹Ocular Wound Healing and Therapeutics, Singapore Eye Research Institute, Singapore; ²Centre for Eye Research Australia, Royal Victorian Eye and Ear Hospital, Melbourne, Australia; ³Glaucoma Service, Singapore National Eye Center, Singapore; ⁴Department of Ophthalmology, Yong Loo Lin School of Medicine, National University of Singapore; and ⁵School of Materials Science and Engineering, Nanyang Technological University, Singapore

Glaucoma is a progressive optic neuropathy, which, if left untreated, leads to blindness. The most common and most modifiable risk factor in glaucoma is elevated intraocular pressure (IOP), which can be managed surgically by filtration surgery. The postoperative subconjunctival scarring response, however, remains the major obstacle to achieving long-term surgical success. Antiproliferatives such as mitomycin C are commonly used to prevent postoperative scarring. Efficacy of these agents has been tested extensively on monkey and rabbit models of glaucoma filtration surgery. As these models have inherent limitations, we have developed a model of glaucoma filtration surgery in the mouse. We show, for the first time, that the mouse model typically scarred within 14 d, but when augmented with mitomycin C, more animals maintained lower intraocular pressures for a longer period of time concomitant with prolonged bleb survival to beyond 28 d. The morphology of the blebs following mitomycin C treatment also resembled well-documented clinical observations, thus confirming the validity and clinical relevance of this model. We demonstrate that the antiscarring response to mitomycin C is likely to be due to its effects on conjunctival fibroblast proliferation, apoptosis and collagen deposition and the suppression of inflammation. Indeed, we verified some of these properties on mouse conjunctival fibroblasts cultured *in vitro*. These data support the suitability of this mouse model for studying the wound healing response in glaucoma filtration surgery, and as a potentially useful tool for the *in vivo* evaluation of antifibrotic therapeutics in the eye.

© 2011 The Feinstein Institute for Medical Research, www.feinsteininstitute.org

Online address: <http://www.molmed.org>

doi: 10.2119/molmed.2010.00188

INTRODUCTION

The most common reason for failure in glaucoma filtration surgery (GFS) is scarring and fibrosis. Subconjunctival scarring at the level of the subconjunctival fibroblasts often leads to poorly filtering blebs and a subsequent rise in intraocular pressure (IOP) (1). To prevent scarring, pharmacological approaches, such as the use of antifibrotic agents, have been attempted in experimental and clinical studies. Drugs with proven efficacy in humans include topical corticosteroids, and intraoperatively applied antiproliferatives such as 5-fluorouracil

(5FU) and mitomycin C (MMC) (2–5). MMC, an antibiotic secreted by *Streptomyces caespitosus*, acts as an alkylating agent that crosslinks DNA, thereby inhibiting DNA synthesis. MMC also inhibits RNA and protein synthesis and it interacts with molecular oxygen, which in turn generates free radical damage to DNA and protein (6). These nonspecific effects are, however, associated with severe and often blinding complications that include hypotonous maculopathy (7), thin, cystic and leaky blebs that are prone to infections, and bleb-related endophthalmitis (8,9). Furthermore, GFS

fails in a substantial number of high-risk eyes despite the use of these antiproliferative agents. As a result, the subject and understanding of the subconjunctival wound healing response is far from complete, and the quest to find a safer alternative and more specific antiscarring agent remains a top priority.

To address this area of research, several animal models, including rat (10,11), rabbit (12–15) and monkey (16,17), have been developed to study the clinical and histological scarring response after GFS. The rabbit has, by far, been the most popular animal used for such studies owing to both the relatively large ocular structures, allowing ease of surgical manipulation, and cost-effectiveness. However, many aspects of GFS cannot be examined in detail in the rabbit owing to the limited availability of reagents such as antibodies, gene expression arrays, and so on. To date, a successful mouse model for GFS has not been described,

Address correspondence and reprint requests to Li-Fong Seet, Singapore Eye Research Institute, 11 Third Hospital Avenue, #06-00 SNEC Building, Singapore 168751. Phone: (65) 63275812; Fax: (65) 63224599; E-mail: seet.li.fong@seri.com.sg; or Tina T Wong, Glaucoma Service, Singapore National Eye Center, 11 Third Hospital Avenue, Singapore 168751. Phone: (65) 63227477; Fax: (65) 62277290; E-mail: tina.t.L.wong@sneec.com.sg.
Submitted October 1, 2010; Accepted for publication January 6, 2011; Epub (www.molmed.org) ahead of print January 11, 2011.

although simplified models for the study of subconjunctival wound healing have been reported previously (18,19). A mouse model of GFS would be invaluable for several reasons. First of all, many critical reagents such as antibodies are available for the mouse to study the wound healing response by histology, flow cytometry, enzyme-linked immunosorbent assay (ELISA), and so on, and *in vivo* ocular imaging techniques are readily accessible. Understanding the wound healing or fibrotic process is crucial to the discovery of novel antifibrotic therapeutics. Secondly, the mapped and sequenced mouse genome makes possible the manipulation of target genes in the mouse, facilitating the design of overexpression DNA constructs, microRNA or small interfering RNA molecules as potential therapeutics to be validated first in the mouse. Thirdly, many potential therapeutics such as neutralizing antibodies or antagonizing reagents specifically for the mouse are available, allowing proof-of-concept experiments to be performed readily. Fourthly, the GFS response in genetically altered animals such as knockouts or transgenic mice can be easily studied.

We have developed a mouse model of GFS which can be employed to investigate the postoperative subconjunctival scarring response (21). To ascertain that the murine model is relevant to the clinical setting, we applied MMC in the mouse model and examined the postoperative surgical responses. MMC is commonly applied intraoperatively to reduce the postoperative scarring response following filtration surgery in patients. We investigated the effect of intraoperative MMC on bleb survival and morphology by incorporating major imaging techniques used in the clinic, including slit lamp examination, anterior segment-optical coherence tomography (AS-OCT) as well as *in vivo* confocal imaging. We also examined the pathohistology of the blebs with and without MMC treatment by polarization microscopy and immunofluorescent analyses. These were further corroborated by *in vitro* studies

using cultured mouse conjunctival fibroblasts. We provide data to show not only the mechanisms whereby MMC may improve surgical success in GFS, but at the same time, the probable reasons for the known side effects attributed to MMC in humans. Most importantly, we demonstrate that our mouse model is suitable, valid and closer to the actual human glaucoma filtration surgery than other hitherto described mouse models of conjunctival wound healing.

MATERIALS AND METHODS

Mouse Model of Glaucoma Filtration Surgery

C57BL/6 mice were bred and maintained at the Singhealth Experimental Medical Centre (Singapore General Hospital, Singapore). All experiments with animals were approved by the Institutional Animal Care and Use Committee (IACUC) and treated in accordance with the Association for Research in Vision and Ophthalmology (ARVO) Statement on the Use of Animals in Ophthalmic and Vision Research. The mice were anesthetized by intraperitoneal (i.p.) injection of a 0.1 mL ketamine/xylazine mixture containing 2 mg/mL xylazine hydrochloride (Troy Laboratories, Smithfield, Australia) and 20 mg/mL ketamine hydrochloride (Ketamine, Parnell Laboratories, Alexandria, Australia) before the operation was carried out. The modified filtering surgery was performed only on the left eye of each mouse as described in the text. MMC (Kyowa Hakko Kirin Co. Ltd, Shizuoko, Japan) was applied at 0.4 mg/mL with a small piece of surgical sponge (MQA, Inami, Tokyo, Japan). Irrigation of the MMC-treated area was performed with 2 mL of 0.9% sodium chloride (B Braun Melsungen AG, Melsungen, Germany) using a syringe. The dissected conjunctiva was secured and closed by an 11-0 (0.1 metric) Ethilon monofilament nylon scleral suture (Ethicon Inc., Somerville, New Jersey, USA). Fucithalamic ointment (Leo Pharmaceutical Products, Ltd, Princes Risborough, Buckinghamshire, UK) was

instilled at the end of the procedure. MMC treatment was performed on eight eyes, and control (without treatment) was performed on 10 eyes.

Measurement of IOP

The mice were anesthetized as described above before IOP measurements. Intraocular pressures were recorded in both eyes of each animal with a handheld commercial rebound tonometer according to instructions by the manufacturer (TonoLab, Icare, Espoo, Finland). All measurements were taken between 4 and 7 min after anesthetic injection, as suggested by a prior study (20); 5 to 10 measurements of IOP in each eye were taken and the mean value of the IOP of the left operated eye is expressed as a percentage over that of the unoperated right eye of the same animal. An IOP that is < 70% of baseline IOP is used as an indicator of effective filtration and bleb function. Eight animals from each group were subjected to IOP measurements.

Detection and Analysis of Blebs

Careful slit lamp, anterior segment-optical coherence tomography (AS-OCT) and *in vivo* confocal microscopic examinations on subconjunctival blebs were performed at postoperative day 2, and weekly thereafter for a total of 4 wks as described previously (21). A bleb was judged to have failed if the surgical site appeared flat by slit lamp analysis. Slit lamp examination was performed by three examiners who were masked to the treatment groups. All animals from each group were subjected to slit lamp and AS-OCT analyses. *In vivo* confocal microscopy was performed on two animals from each group as described previously (21).

Histology and Immunofluorescent Analyses

Mice were euthanized on day 28 after surgery, and the eyes were enucleated for immediate fixation and processing as described (21). Five- μ m sections were stained with hematoxylin and eosin to visualize tissue morphology. To assess the

collagen matrix, picrosirius red staining was performed as described previously (22) and visualized by polarization microscopy (Olympus BX51, Olympus, Center Valley, PA, USA). For immunofluorescent analysis, antibodies specific for collagen (Abcam plc, Cambridge, UK), Ki67 (Abcam plc), CD45 (BD Pharmingen, Lexington, KY, USA), CD11b (Chemicon, Temecula, CA, USA) and α -SMA (Abcam plc) were used. The primary antibodies were visualized using secondary antibodies conjugated to either AlexaFluor-488 or AlexaFluor-594 (Invitrogen, Eugene, OR, USA). Sections were visualized using the Zeiss Imager.Z1 microscope (Carl Zeiss MicroImaging GmbH, Göttingen, Germany). Histology was performed on three eyes from each group.

Terminal Deoxynucleotidyl Transferase dUTP Nick End Labeling (TUNEL) Analysis

End labeling of exposed 3'-OH ends of DNA fragments in cryosections and cultured mouse conjunctival fibroblasts was performed with the DeadEnd Fluorometric TUNEL System according to manufacturer's instructions (Promega, Madison, WI, USA). Staining of the cell nucleus was achieved by mounting the TUNEL-stained cryosections or fibroblasts in DAPI-containing Vectashield mounting medium (Vector Laboratories, Burlingame, CA, USA). Sections and cells were visualized using the Zeiss Imager.Z1 microscope (Carl Zeiss Inc.).

Cell Culture and Treatment with MMC

Conjunctival fibroblasts obtained from C57BL6/J mice were cultured as described previously (21). For treatment with MMC, cells were treated with a single application of 0.4 mg/mL MMC for 1 min. After treatment, cells were washed 3 \times with phosphate-buffered saline (PBS) (Invitrogen) and maintained in culture medium for 72 h before analyses.

Real-Time Cell Proliferation Analysis

The xCelligence real-time cell analyzer (Roche Diagnostics GmbH, Penzberg, Germany) was used to assess cell prolifer-

ation according to manufacturer's instructions. Mouse conjunctival fibroblasts were trypsinized and seeded at 8,000 cells per well in an E-Plate 96 (Roche) in quadruplicates. For cells treated with MMC, drug treatment was performed at 0.4 mg/mL for 1 min on trypsinized cells followed by three washes in PBS before being seeded onto the wells at 8,000 cells/well in normal culture medium. The plated cells were allowed to equilibrate for at least 30 min in the tissue culture incubator before electrode resistance was recorded. Cell growth was monitored continuously for up to 6 d.

RNA Isolation and Expression

Total RNA recovery, first-strand cDNA synthesis and quantitative real-time PCR (qPCR) was performed as described previously (21). All PCR reactions were performed in triplicate. All mRNA levels were measured as C_T threshold levels and were normalized with the corresponding β -actin C_T values. Values were expressed as fold increases over the corresponding values for untreated control by the $2^{\Delta\Delta C_T}$ method. The primers for collagen I α 1 and β -actin were as described previously (21). The presented data is representative of three independent experiments.

Statistical Analysis

All data were expressed as mean \pm standard deviation (SD) where appropriate. Survival analysis was performed for bleb failure using the Kaplan-Meier log-rank test. The significance of differences among groups was determined by the one-tailed Student *t* test using the Microsoft Excel 5.0 software. $P < 0.05$ was considered statistically significant.

RESULTS

A Murine Model of Glaucoma Filtration Surgery

Modified filtering surgery in the mouse was undertaken on the left eye as described previously (21) (Figure 1). The goal of the surgery was to create a fistula through the sclera to facilitate the outflow of aqueous humor from the anterior

chamber into the subconjunctival space, and thereby cause a reduction in the IOP.

MMC Treatment Was More Effective in Lowering IOP

Absolute IOP values do not take into account IOP variability of the individual mouse, as was observed in humans (23). To better assess the impact of the surgery on IOP, we expressed the IOP of the operated left eye as a percentage of the IOP of the unoperated right eye of each animal at each time point measurements were taken. Errors arising from variability in individual baselines are thus eliminated and the presented data is reflective of the IOP alteration from the baseline that is characteristic of each animal as a result of the surgery. As shown in Figure 2A, the mean % IOP of the operated versus the paired unoperated eye in the control animals reduced from 99% \pm 14% on day 7 to 65% \pm 20% on day 14, and then rose back up to 84% \pm 28% on day 21 and 85% \pm 14% on day 28. This profile suggests that a reduction in IOP in the operated eyes is maximal in the second week after surgery with a return to baseline thereafter. Treatment with MMC produced a sustained reduction in the IOP of the operated mice, with the mean % IOP dropping to 70% \pm 21% on day 7, and this was maintained for the next 3 wks (% IOP = 71% \pm 16%, 74% \pm 19% and 75% \pm 26% on days 14, 21 and 28 respectively). Since a target pressure of 20% to 30% lower than baseline is recommended for most glaucoma patients (23), we analyzed the efficacy of MMC treatment in this model in achieving a 30% reduction from baseline IOP (equivalent to a % IOP of operated versus unoperated eye of 70%). As shown in Figure 2B, MMC treatment resulted in 50% of the operated mice compared with none in the control group achieving an IOP that was 70% of the baseline IOP on day 7. At day 14, an equal number of the control or MMC-treated animals had a 30% reduction in IOP (50% in each group). In the third and fourth week after surgery, twice more MMC-treated animals achieved a 30% IOP reduction compared with control animals. The number of eyes exhibiting a

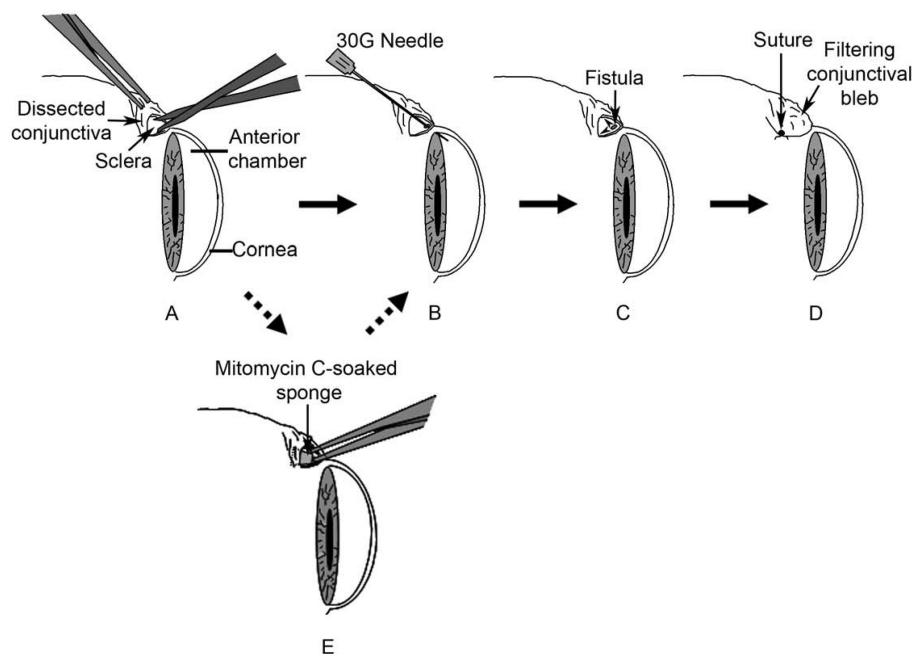


Figure 1. A murine model of glaucoma filtration surgery. Schematic diagram depicting the surgical process in the mouse eye. The conjunctiva was dissected so as to expose the sclera and a small filtration subconjunctival space was created by running the surgical scissors underneath the dissected conjunctiva (A). An incision was then made with a 30-gauge needle through the sclera into the anterior chamber of the eye to create a fistula (B) so as to allow aqueous humor to exit from the anterior chamber and into the subconjunctival space (C). The final surgical step involved suturing the dissected conjunctiva over the newly created fistula (D). For the MMC treatment arm, 0.4 mg/mL MMC was applied between the sclera and the dissected conjunctiva using a small section of surgical sponge for 1 min (E). After the sponge was removed, the area was irrigated with 0.9% sodium chloride before cannulation of the sclera (B) and the final suturing of the conjunctiva (D). This figure is modified from a similar figure published previously (21).

reduction in IOP to less than 70% of the unoperated baseline is maximal on day 14 (4 of 8 eyes) in control eyes and day 21 in MMC-treated eyes (6 of 8 eyes) and this is evident as a shift in the profile in Figure 2B. MMC treatment is thus more effective than control in achieving a higher frequency of a reduction in IOP by 30% or more.

MMC Prolonged Bleb Survival

Filtration of fluid from the anterior chamber through the surgically created fistula into the subconjunctival space is obvious as an elevated conjunctival bleb. The raised, filtering blebs were conspicuous in the initial 48 h following surgery in both the control and MMC-treated eyes, as analyzed by slit lamp microscopy

(Figure 3A). While the blebs in the MMC-treated eyes remained obvious on day 7 after surgery, the blebs in the control eyes became less elevated and noticeably more vascularized. By day 14 after surgery, there was no obvious filtering bleb in the control eyes, as evidenced by the flattened, vascularized conjunctiva at the site where the bleb was previously noted. In contrast, the MMC-treated eyes retained the presence of a bleb that appeared cystic and less vascularized on day 28. Indeed, a significant difference in bleb survival was observed between the two groups (log rank; $P = 0.013$; Figure 3B). With MMC, 6 of 8 blebs (75%) survived at day 28. This is in contrast to control eyes where only 1 of 10 blebs (10%) survived at the end of the study. No significant ad-

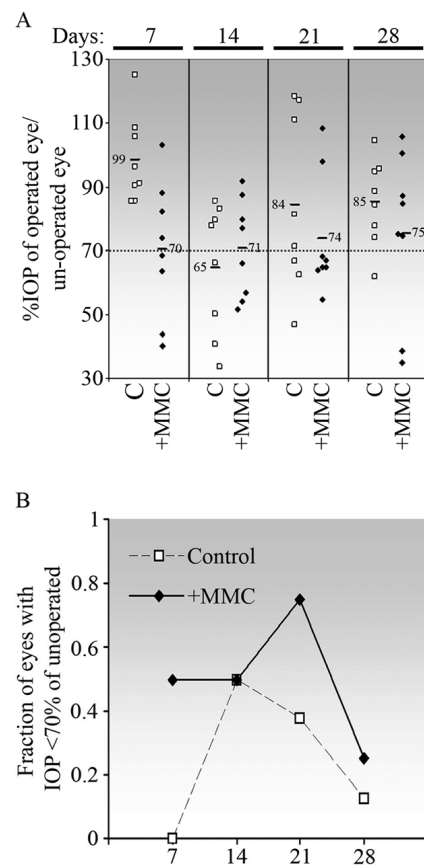


Figure 2. Increased number of eyes with intraoperative episcleral application of MMC maintained a lower IOP than control eyes. (A) The IOPs of both operated and unoperated eyes of each animal at the indicated postsurgery day were measured at least five times. Each value represents the % mean IOP of the operated eye over the mean IOP of the unoperated eye of the same animal at each time point measurements were taken. Each symbol represents a single animal (\square , control, $n = 8$; \blacklozenge , MMC-treated, $n = 8$). The horizontal bars and numbers indicate the mean % IOP. Dotted line indicates the 70% IOP level. C indicates control. (B) Graphical representation of the fraction of eyes with IOP maintained at less than 70% of the unoperated IOP of the same animal as a function of time after surgery. The values were calculated on the basis of panel A.

verse clinical complications or MMC toxicity such as corneal erosion, corneal opacification, cataract, endophthalmitis, or moderate to severe inflammation on

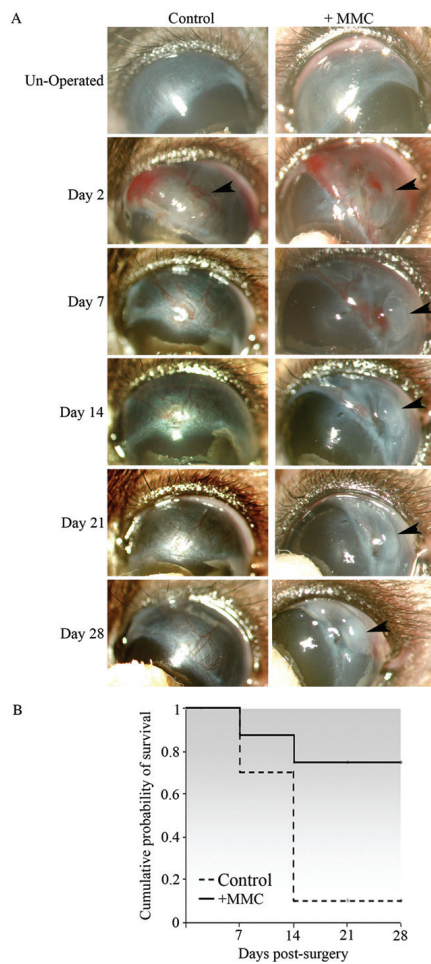


Figure 3. Augmentation of glaucoma filtration surgery with MMC prolonged bleb survival. (A) Slit lamp examination of the surgical sites revealed the presence of the blebs (arrowheads) in the conjunctiva of the operated eyes. Ten control and eight MMC-treated eyes were examined. (B) Kaplan-Meier survival curve showing that survival rates of filtering bleb were improved with MMC treatment. Bleb survival was determined on the basis of slit lamp examination as shown in (A). Ten control eyes and eight MMC-treated eyes were scored, $P = 0.013$ (Kaplan-Meier log-rank test).

the sclera, were recorded in any of the eyes from each group.

Further analysis by anterior segment-optical coherence tomography (AS-OCT) was performed to evaluate bleb survival. OCT measurements on days 2, 7, 14, and 28 after surgery confirmed the slit lamp

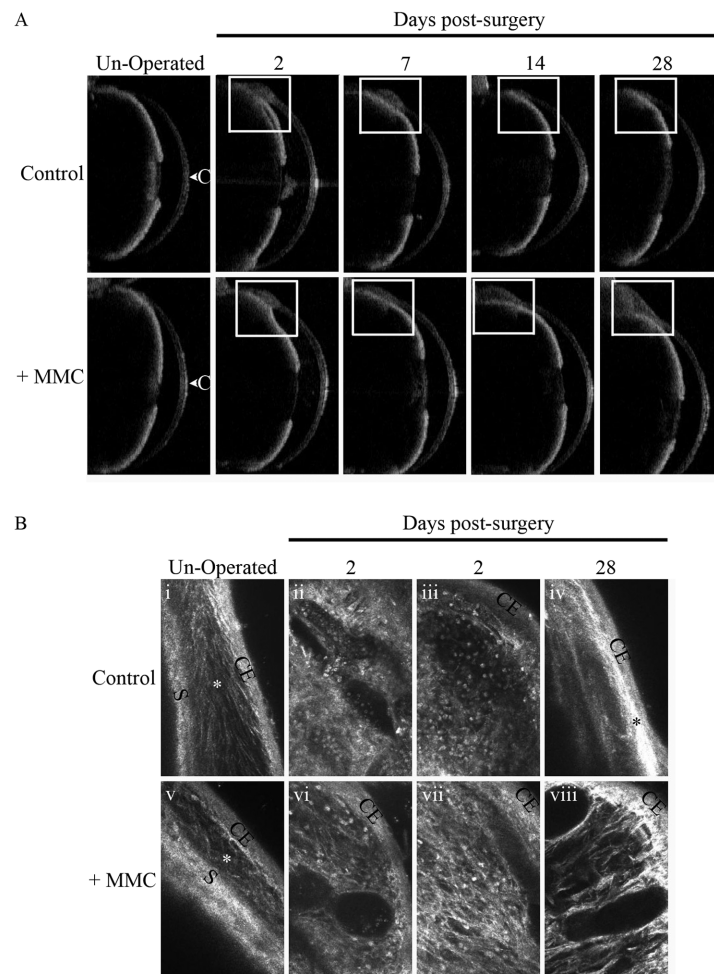


Figure 4. *In vivo* imaging of the surgical sites. (A) Anterior segment optical coherence tomography imaging of the mouse conjunctiva. The unoperated and operated eyes on days 2, 7, 14 and 28 were examined. The location of the bleb is indicated by the white box. Images shown belong to the same control or MMC-treated eye over the time course of the analysis. Ten control eyes and eight MMC-treated eyes were examined. C indicates cornea. (B) *In vivo* confocal microscopy images of the blebs. (i, v) The subconjunctival matrix of the unoperated eye is indicated by a white *. Numerous microcysts in the conjunctival matrix can be observed in both control (ii) and MMC-treated (vi) eyes 2 d after surgery. While the dull microdots in the control eye are likely to be inflammatory cells derived from the surrounding vascular or lymphatic network (iii), MMC treatment is associated with the presence of hyperreflective microdots, which may represent necrotic epithelial cells (vii). (iv) By day 28 in the control eye shown, the operated site appeared scar-like with a dense connective tissue with few or no clear spaces (black *). (viii) The MMC-treated operated site maintained numerous microcysts although some encapsulation may be present at the periphery of the bleb. Two eyes from each group were examined. CE, conjunctival epithelium; S, sclera.

observations (Figure 4A). The bleb in a representative control operated eye can be observed to reduce progressively in size until its complete disappearance by day 14. In contrast, the bleb in a representative MMC-treated eye remained vis-

ible on each of the indicated days for 28 d (see Figure 4A).

In vivo confocal microscopy of the control blebs on day 2 revealed the presence of optically clear spaces filled with fluid (Figure 4B, ii) which were absent in the

unoperated eye (Figure 4B, i). These spaces may correspond with microcysts which were reported to be numerous in functioning human blebs (24). The subconjunctival connective tissue also appeared to be arranged loosely in the control day 28 bleb (Figure 4B, ii, iii). Likewise, we observed numerous well-defined clear spaces in the blebs of the MMC-treated eyes that are reminiscent of microcysts (Figure 4B, vi, vii). Interestingly, we also observed the presence of hyperreflective microdots in the bleb of the MMC-treated eye (see Figure 4B, vii). On day 28, the subconjunctival space in the flattened bleb area of the control eye was observed as an optically dense, fibrotic connective tissue with no clear spaces (Figure 4B, iv). In contrast, relatively large microcystic spaces remained in the bleb of the MMC-treated eye and these were surrounded by loosely organized connective tissue (Figure 4B, viii). Optically dense fibrotic tissue adjunct to the conjunctival epithelium that is evocative of encapsulation was also observed in the MMC-treated bleb (see Figure 4B, viii).

MMC Reduced Collagen Deposition in the Bleb

We next investigated the histopathological differences underlying the wound response between control and MMC-treated eyes at day 28 after surgery. The control surgical site comprised of thick strands of fibrous material in the subconjunctival space overlying the sclera, which consisted of even denser and more tightly packed connective tissue (Figure 5A, B). In comparison, the surgical site in the MMC-treated eye was vacuous and punctuated with thin, fine strands of connective tissue fibrils (Figure 5C, D). These observations suggest that collagen deposition might be altered in the MMC-treated eyes.

To assess the collagen deposition in the control versus MMC treatment, we performed sirius red polarization microscopy on the tissue sections. Indeed, the surgical site in the control eye was densely compacted with thick, well-aligned collagen fibers resembling a scar

(Figure 5E, F). Moreover, the control wound site showed a predominance of mature collagen fibers which were orange-red birefringent (see Figure 5F). In contrast, the bleb in the MMC-treated eyes contained few and thin, loosely assembled collagen fibers in an expanded noncollagenous subconjunctival space (Figure 5G, H). The majority of the collagen fibers also were noticeably yellow-

green birefringent in the MMC-treated bleb, suggesting the preponderance of immature fibers (see Figure 5H). Thus, the survival of the bleb in the MMC-treated eye is, in part, due to reduced deposition of collagen fibers and deficient maturation of the scar at the wound site.

To further determine differences in the extracellular matrix of the control and MMC-treated conjunctiva, immuno-

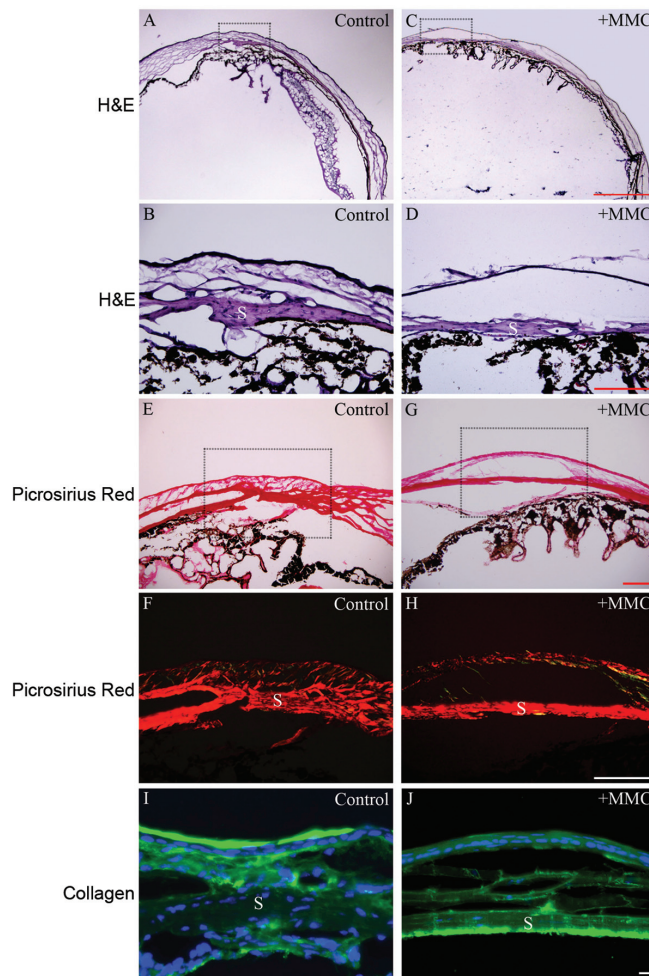


Figure 5. MMC reduced collagen deposition at the surgical site. (A,C) Hematoxylin and eosin (H&E) staining revealed a flattened conjunctiva at the day-28 control operated site (boxed area) whereas the MMC-treated operated site subconjunctival space was expanded with an almost clear matrix (boxed area); scale bar, 500 μ m. (B,D) Higher magnification of insets (boxed areas in A and C respectively); scale bar, 100 μ m. (E,G) Picrosirius red-stained sections of the same eyes at low magnification and visualized by brightfield microscopy; scale bar, 100 μ m. (F,H) Higher magnification of insets (boxed areas in E and G respectively) and polarization microscopy revealed differences in the collagen matrices of the control versus MMC-treated eye; scale bar, 100 μ m. (I,J) Immunofluorescence analysis of sections from the same eyes with a collagen I-specific antibody; scale bar, 10 μ m. S, sclera.

fluorescence analysis for collagen expression was carried out. The control-operated conjunctiva exhibited more enhanced staining for collagen I in the subconjunctival space (Figure 5I) when compared with the MMC-treated counterpart (Figure 5J).

MMC Inhibited Proliferation and Induced Apoptosis in the Mouse Operated Conjunctiva

The presence of proliferative cells at the surgical site was visualized by immunostaining the cryosections with antibodies against Ki67 (25). Surprisingly, at day 28 after surgery, Ki67-positive cells can be observed close to the edge of the wound in the control conjunctival epithelium, suggesting that there are possibly wound-activated proliferating cells remaining at the surgical site (Figure 6A, upper panel, arrowheads). As expected, there were no visible proliferating cells at the MMC-treated wound site (Figure 6A, bottom panel).

To determine the induction of apoptosis by MMC, cryosections were subjected to TUNEL staining. The control conjunctiva did not present with any TUNEL-positive cells (Figure 6B, upper panel). In striking contrast, almost all of the cells in the conjunctival epithelium as well as cells in the subconjunctival space and those abutting the episclera were apoptotic in the MMC-treated surgical site (Figure 6B, lower panel, arrowheads). This finding raises concern about tissue recovery, especially of the conjunctival epithelium, since the presence of apoptotic cells here seemed to persist for at least 28 d after surgery and there were no apparent proliferative cells to repair eventual cell loss due to apoptosis.

MMC Suppressed the Recruitment of Inflammatory Cells to the Surgical Site

The influx of inflammatory cells to the surgical site is a wound healing response associated with fibrosis. To examine this, tissue sections were subjected to immunostaining for CD45 and CD11b expressions. CD45, present on the surface of nucleated cells including B cells,

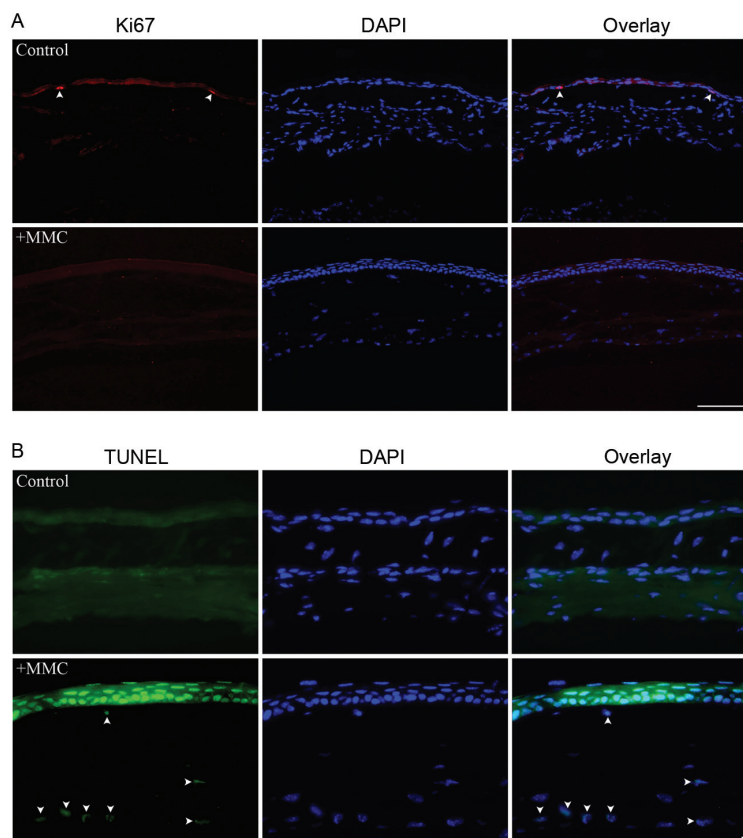


Figure 6. Cell death in the conjunctiva and episclera after MMC treatment. (A) Tissue sections were stained with Ki-67 (red) to visualize proliferating conjunctival epithelial cells in the control operated eye (arrowheads) versus the absence of any detectable proliferating cells in the MMC-treated operated eye; scale bar, 100 μ m. (B) No apoptotic (TUNEL-positive) cells, which would have appeared as bright green cells, were seen in the control operated site, while many apoptotic cells were observed in the conjunctival epithelium as well as the episclera at the MMC-treated surgical site (arrowheads); scale bar, 10 μ m.

T cells, neutrophils and macrophages of hematopoietic origin, is commonly used as a marker for inflammation (26). The conjunctival epithelium, subconjunctival space as well as the most anterior cell layer of the sclera at the wound site of the control eye revealed positive staining for CD45 (Figure 7A, arrowheads). In contrast, CD45 expression was detected mainly in the more posterior cell layers of the sclera in the bleb of the MMC-treated eye (Figure 7B, arrowheads). CD11b, a cell surface marker expressed at high levels on macrophages and monocytes (27), was found to be expressed in the episclera of the control wound site (Figure 7C, arrowheads) but absent in the MMC-treated eye (Figure 7D). These

observations may be explained by the possibility that MMC caused the loss of normal conjunctival and episcleral vasculatures so that recruitment of CD45⁺ and CD11b⁺ cells to the conjunctival epithelium and episclera was suppressed. To examine this possibility, we carried out immunofluorescent analysis of consecutive tissue sections with antibodies against α -SMA. First of all, we did not observe any fibroblasts in the conjunctiva expressing this marker in either control or MMC-treated eyes. This is possibly due to the fact that by day 28, the wound healing process is at a late stage, and α -SMA-positive myofibroblasts are known to be lost after the early active period of wound contraction (28,29). In-

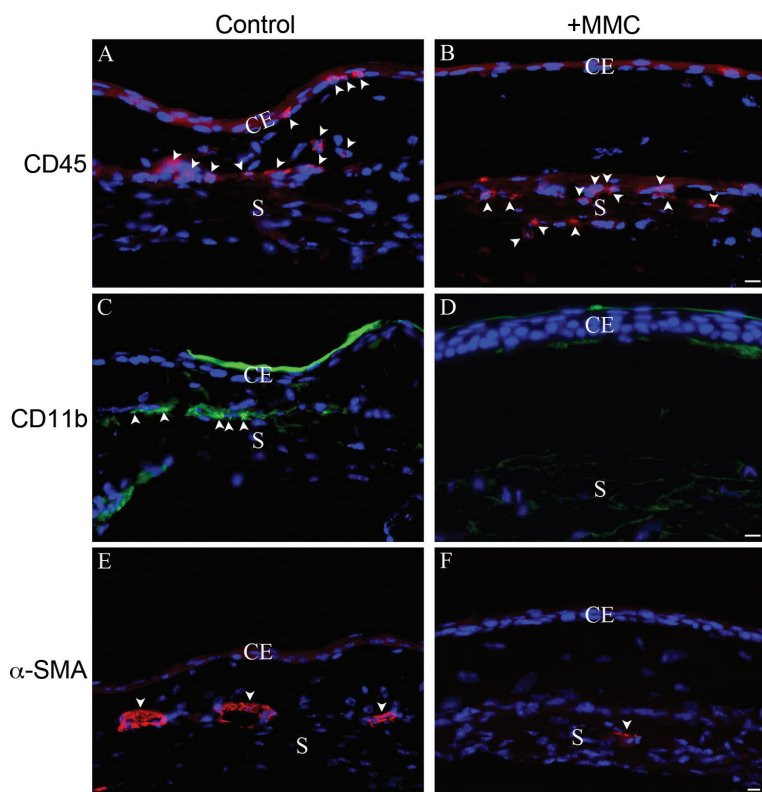


Figure 7. Recruitment of inflammatory cells to the operated site of control versus MMC-treated eyes. (A,B) Immunostaining for CD45⁺ leukocytes revealed the presence of these cells in the conjunctival epithelium and episclera region of the control operated area (A, arrowheads) while in the MMC-treated operated site, they were detected mainly in the posterior scleral cell layers (B, arrowheads). (C,D) Immunostaining with the CD11b antibody showed that inflammatory cells were present in the episclera area of the control operated site (C, arrowheads) while CD11b-positive inflammatory cells were absent in the MMC-treated operated area. (E,F) α -SMA-positive cells present in the episcleral area of the control operated site may represent pericytes surrounding vascular vessels (E, arrowheads) which in the MMC-treated eye were present only in the posterior scleral cell layers at the surgical site (F, arrowhead). CE, conjunctival epithelium; S, sclera. Scale bar, 10 μ m.

stead, we observed α -SMA-positive cells present around structures that resembled blood vessels (Figure 7E, F, arrowheads). α -SMA is known to be expressed by perivascular mural cells or pericytes (30). Interestingly, the locations of these potential blood vessels were close to the episclera in the control surgical site (Figure 7E). This would account for the presence of inflammatory cells near the episclera of the surgical site in the control eye. In contrast, we observed few α -SMA-positive blood vessel-like structures in the MMC-treated sclera and, when they could be observed, they ap-

peared to exist in the deeper more posterior scleral layers (Figure 7F, arrowhead). This may explain why CD45⁺ cells were observed mainly in the more posterior scleral layers and not in the episclera of the MMC-treated site.

MMC Inhibited Proliferation, Induced Apoptosis and Inhibited Collagen I α 1 Expression in Cultured Mouse Conjunctival Fibroblasts

To verify the mechanism of action of MMC deduced from the *in vivo* observations described above, as well as to determine if the observed *in vivo* effects

parallel the *in vitro* cellular response to MMC treatment, we performed a series of experiments on cultured mouse conjunctival cells. Using the real time cell analyzer (RTCA) SP instrument (31), we analyzed conjunctival cell growth after MMC treatment in comparison to control untreated cells. Cell index values produced by the MMC-treated cells indicated the lack of proliferation, while the cell index values of the control cells increased progressively with time (Figure 8A). Hence, a single application of MMC was able to suppress the growth of the mouse conjunctival fibroblasts effectively for up to 6 d. The lack of proliferation was verified by the lack of Ki67 positive staining in cells that were treated with MMC (Figure 8B, lower panel) compared with control cells (Figure 8B, upper panel). When analyzed by TUNEL staining, only a small number of MMC-treated cells were observed to be apoptotic (Figure 8C, lower panel, arrowheads) while none were observed in the control (Figure 8C, upper panel). This was surprising considering that most of the cells in the MMC-treated conjunctiva *in vivo* appeared TUNEL positive. The MMC-treated cells also were examined for the expression of collagen I α 1 mRNA by qPCR. MMC treatment significantly and consistently reduced collagen I α 1 mRNA expression compared with control (Figure 8D).

DISCUSSION

We confirm in this study the validity of a model for GFS in the mouse. To our knowledge, the closest known mouse model for GFS is a simple conjunctival scarring model where a fixed volume of saline was injected into the subconjunctival space to create a visible bleb (19). Our model is significantly closer to the surgical procedure, known as a trabeculectomy that is performed on human eyes. The major surgical endpoint of a trabeculectomy is a filtering bleb allowing aqueous humour to flow from the anterior chamber into the subconjunctival space. This endpoint is achieved with our mouse model. The only major differ-

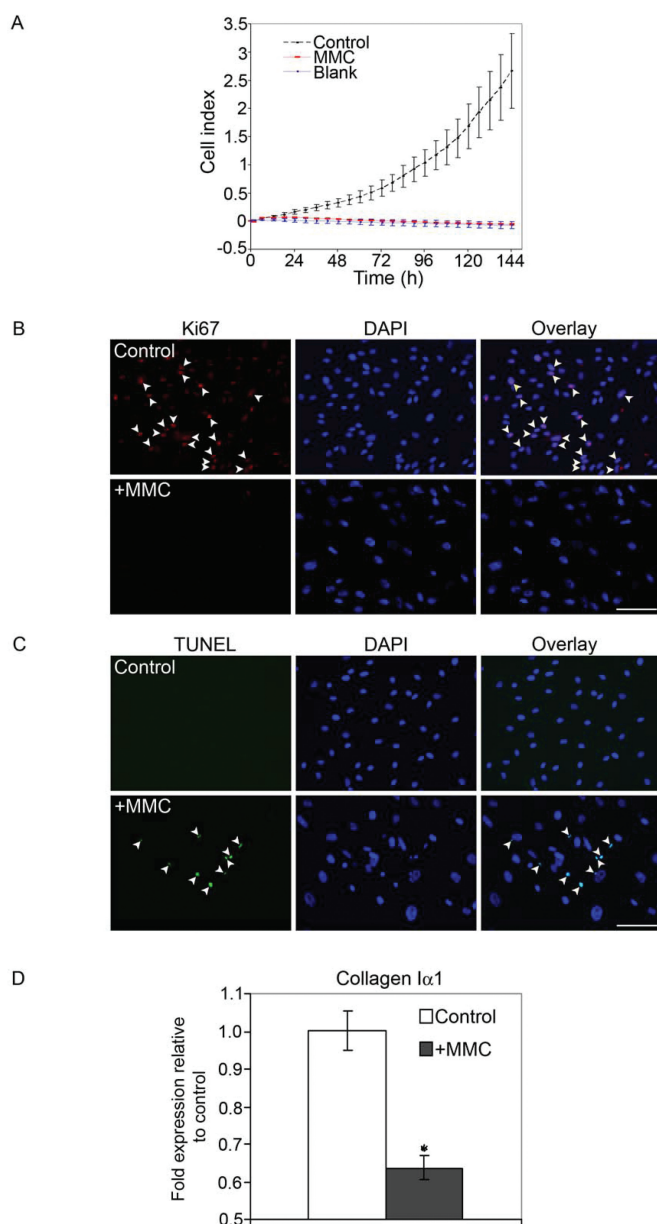


Figure 8. MMC effects on mouse conjunctival cell proliferation, apoptosis and collagen $\alpha 1$ expression. (A) Cell growth was monitored continuously using the RTCA SP instrument. The cell index profiles of untreated cells (dotted black line) and MMC-treated cells (red line) reflect the logarithmic growth phase and response to treatment respectively. The cell index values for MMC-treated cells did not demonstrate a logarithmic growth phase that was measured for the control cells indicating that the treated cells did not proliferate. (B) Cells were treated with MMC for 1 min and maintained in culture medium for 72 h before staining with DAPI (blue) and anti-Ki67 antibody (red). Selected cells that are positive for Ki67 are indicated by arrowheads; scale bar, 100 μm . (C) Cells were treated as in (B) and analyzed by TUNEL staining (green). Nuclei were visualized by DAPI staining (blue). Cells positive for TUNEL staining are indicated by arrowheads; scale bar, 100 μm . (D) Cells were treated the same as in (B) and assayed for collagen $\alpha 1$ mRNA abundance by real-time quantitative PCR. MMC treatment significantly reduced the amount of collagen $\alpha 1$ mRNA by 40% compared with untreated control cells ($P = 1.8 \times 10^{-10}$). Bars represent the SD. Data shown is representative of three independent experiments.

ence in the mouse surgical model is that, unlike in trabeculectomy, a partial thickness guarded scleral flap is not created owing to the very thin sclera of the mouse eye, causing this step of the operation to be technically and surgically very challenging. Therefore needle tract sclerostomy, which scarred in 14 days, was performed instead, as described in this study. The intraoperative application of MMC extended the bleb survival period to beyond 28 days, supporting the use of this drug in the clinic to improve surgical success. We also demonstrated that treatment with MMC resulted in a higher frequency of surgical success based on maintenance of an IOP below 70% of baseline. These two MMC-induced effects in our mouse model parallel those observed previously in the rabbit (32) and the monkey (33) models. Furthermore, alterations in the *in vivo* bleb structure in our model were reminiscent of those observed previously in the clinic (24). Histologic features also mirrored those observed in the clinic with reduced matrix deposition in the MMC eyes compared with the control eyes. Given the close correlation with documented clinical response, our model is ideal not only for studying the healing and fibrotic processes that are activated following surgery, but also for delineating the mode of drug action.

In the present study, we evaluated the effect of MMC on three aspects of conjunctival wound healing in the mouse GFS model: cell proliferation, deposition of collagen and inflammation in the wound bed. As in trabeculectomies (34), the majority of the scarring effects in our mouse model were observed at the level of the episclera and the subconjunctival space.

The profound cytotoxic effect of MMC in the proliferation phases of Tenon's fibroblasts (35–37) was demonstrated clearly in our model where the MMC-treated conjunctiva contained no detectable proliferative cells compared with the control wound site, which did contain proliferative cells. Mouse conjunctival fibroblasts cultured *in vitro* showed

the same antiproliferative response to MMC. It has been suggested that MMC prevents the recruitment and activation of conjunctival fibroblasts through the induction of apoptosis in these cells (38). Indeed, the majority of the cells in the MMC-treated conjunctival epithelium, subconjunctival space, as well as the sclera at the wound site, were apoptotic, which was not the case with the control wound site. The apoptotic effect of MMC also was observed in cultured mouse conjunctival fibroblasts. However, not all the cells cultured *in vitro* were apoptotic, as was also observed in an earlier study on human Tenon fibroblasts (38). Thus, the question arises as to whether activated conjunctival fibroblasts, which cultured cells essentially represent, being devoid of inhibitory compact surroundings, are less sensitive to MMC. This is clinically important because, if MMC causes indiscriminate apoptosis in both activated and inactivated cells, the loss of conjunctival epithelial and fibroblast cells may cause detrimental conjunctival thinning after a single application. Our observation confirms a previous report that MMC effects on rabbit subconjunctival and scleral fibroblast growth was maintained 30 days after GFS (39). This may explain why the use of MMC clinically increases the likelihood that blebs will become thin and cystic, which in turn leads to a lifelong risk of conjunctival breakdown, aqueous humour leakage and bleb-related infections and endophthalmitis (40). Hence, although it has been reported that MMC disappears rapidly from the ocular tissue and that concentration of the agent is reduced significantly by irrigating the tissue copiously immediately after its application (37), the mouse model suggests that long-term effects of MMC *in vivo* should be investigated in detail.

MMC is also thought to inhibit collagen deposition and disorganization, a major phenomenon in fibrosis, by the induction of apoptosis of conjunctival fibroblasts (38). While this may definitely play a part *in vivo*, we showed in this study that MMC treatment may also sup-

press collagen I expression independent of apoptosis *in vitro*. We believe that apoptotic cells, which were fairly low in numbers *in vitro* based on TUNEL staining, could not have been the cause for the significant reduction in collagen I mRNA expression in the presence of MMC. We speculate that MMC may affect collagen I expression via a distinct pathway. Further work is required to address this issue since regulation of collagen production and organization is key to the inhibition of fibrosis in the conjunctiva (21).

The avascular MMC-treated blebs observed in our model suggest that the inflammatory response, which is linked to fibrosis, may be dampened in the MMC-treated eyes. Indeed, we observed fewer persisting inflammatory cells at the operated site after MMC treatment compared with control eyes. We believe this is due in part to the suppression of angiogenesis at the wound site by MMC, which is known to have potent antiangiogenic properties (39). While a microvascular network was apparent around the operated site soon after wounding in the control mouse eye, the MMC-treated blebs were characterized by the lack of vasculature which corresponded with similar observations in the clinic (41). The suppression of angiogenesis is, however, a double-edged sword. On the one hand, inhibiting angiogenesis may limit tissue scarring, but on the other, the lack of a protective inflammatory response stemming from lack of vasculature may contribute to an increased risk of infection at the operated site.

In conclusion, this study has demonstrated that MMC can delay wound healing or fibrosis by mechanisms beyond the inhibition of proliferation. However, the sustained apoptotic effect of MMC on the conjunctival epithelium, subconjunctiva and episclera should be cause for concern particularly with respect to conjunctival breakdown and risk of infection in the long term when used in conjunction with GFS. Finally, the comparable similarities between the clinical effects of MMC and that observed in our mouse

model not only highlighted the suitability of this model for studying the surgical response to known therapeutics but also indicated the application of this model as an invaluable platform for an in-depth understanding of the wound healing response *per se* which will in turn facilitate the discovery and testing of novel antifibrotics.

ACKNOWLEDGMENTS

We thank Hla Myint Htoon (Singapore Eye Research Institute) for help with the statistical analysis and the Department of Pathology, Yong Loo Lin School of Medicine, National University of Singapore, for help with the polarizing microscopy. This work was supported by the National Research Foundation Council Translational and Clinical Research (TCR) Programme Grant (NMRC/TCR/002-SERI/2008) and a research grant from the National Medical Research Council (NMRC/EDG/0019/2008) to TT Wong.

DISCLOSURES

The authors declare that they have no competing interests as defined by *Molecular Medicine*, or other interests that might be perceived to influence the results and discussion reported in this paper.

REFERENCES

1. Hitchings RA, Grierson I. (1983) Clinicopathological correlation in eyes with failed fistulizing surgery. *Trans. Ophthalmol. Soc. U. K.* 103:84-8.
2. Starita RJ, Fellman RL, Spaeth GL. (1985) Short- and long-term effects of postoperative corticosteroids on trabeculectomy. *Ophthalmol.* 92:938-46.
3. Roth SM, Spaeth GL, Starita RJ, Birbillis EM, Steinmann WC. (1991) Effects of postoperative corticosteroids on trabeculectomy and the clinical course of glaucoma. The five-year follow up study. *Ophthalmic Surg.* 22:724-9.
4. The Fluorouracil Filtering Surgery Study Group. (1989) Fluorouracil filtering surgery study one-year follow-up. *Am. J. Ophthalmol.* 108:625-35.
5. Bergstrom TJ, Wilkinson WS, Skuta GL, Watnick RL, Elnor VM. (1991) The effects of subconjunctival mitomycin C on glaucoma filtration surgery in rabbits. *Arch. Ophthalmol.* 109:1725-30.
6. Chabner BA, et al. (2006) *Antineoplastic Agents*. In: *Goodman and Gilman's The Pharmacological Basis of Therapeutics*. 11th ed. Brunton LL (ed.) McGraw-Hill, New York, pp. 1315-403.

7. Jampel HD, Pasquale LR, DiBernardo C. (1992) Hypotony maculopathy following trabeculectomy with mitomycin C. *Arch. Ophthalmol.* 110:1049–50.
8. Greenfield DS, et al. (1996) Endophthalmitis after filtering surgery with mitomycin. *Arch. Ophthalmol.* 114:943–9.
9. Higginbotham EJ, et al. (1996) Bleb-related endophthalmitis after trabeculectomy with mitomycin C. *Ophthalmol.* 103:650–6.
10. Sheridan CM, et al. (1996) Macrophages during fibrosis following scleral fistulizing surgery in a rat model. *Curr. Eye Res.* 15:559–68.
11. Sherwood MB, Esson DW, Neelakantan A, Samuelson DA. (2004) A new model of glaucoma filtering surgery in the rat. *J. Glaucoma.* 13:407–12.
12. Miller MH, Grierson I, Unger WI, Hitchings RA. (1989) Wound healing in an animal model of glaucoma fistulizing surgery in the rabbit. *Ophthalmic Surg.* 20:350–7.
13. Doyle JW, Sherwood MB, Khaw PT, McGrory S, Smith MF. (1993) Intraoperative 5-fluorouracil for filtration surgery in the rabbit. *Invest. Ophthalmol. Vis. Sci.* 34:3313–9.
14. Esson DW, et al. (2004) Expression of connective tissue growth factor after glaucoma filtration surgery in a rabbit model. *Invest. Ophthalmol. Vis. Sci.* 45:485–91.
15. Wong TT, Mead AL, Khaw PT. (2005) Prolonged antiscarring effects of ilomastat and MMC after experimental glaucoma filtration surgery. *Invest. Ophthalmol. Vis. Sci.* 46:2018–22.
16. Hasty B, Heuer DK, Minckler DS. (1990) Primate trabeculectomies with 5-fluorouracil collagen implants. *Am. J. Ophthalmol.* 109:721–5.
17. Bair JS, Chen CW. (1997) Trabeculectomy with multiple applications of mitomycin-C in monkeys with experimental glaucoma. *J. Ocul. Pharmacol. Ther.* 13:115–28.
18. Mietz H, Chevez-Barríos P, Lieberman MW. (1998) A mouse model to study the wound healing response following filtration surgery. *Graefes Arch. Clin. Exp. Ophthalmol.* 236:467–75.
19. Reichel MB, et al. (1998) New model of conjunctival scarring in the mouse eye. *Br. J. Ophthalmol.* 82:1072–7.
20. Haddadin RI, et al. (2009) SPARC-null mice exhibit lower intraocular pressures. *Invest. Ophthalmol. Vis. Sci.* 50:3771–7.
21. Seet LF, et al. (2010) SPARC deficiency results in improved surgical survival in a novel mouse model of glaucoma filtration surgery. *PLoS One.* 5:e9415.
22. Junqueira LCU, Bignolas G, Brentani RR. (1979) Picrosirius staining plus polarization microscopy, a specific method for collagen detection in tissue sections. *Histochem. J.* 11:447–55.
23. Goldberg I. (2003) Relationship between intraocular pressure and preservation of visual field in glaucoma. *Surv. Ophthalmol.* 48(Suppl 1):S3–7.
24. Labbé A, Dupas B, Hamard P, Baudouin C. (2005) In vivo confocal microscopy study of blebs after filtering surgery. *Ophthalmol.* 112:1979–86.
25. Gerdes J, et al. (1984) Cell cycle analysis of a cell proliferation-associated human nuclear antigen defined by the monoclonal antibody Ki-67. *J. Immunol.* 133:1710–5.
26. Hermiston ML, Xu Z, Weiss A. (2003) CD45: a critical regulator of signaling thresholds in immune cells. *Annu. Rev. Immunol.* 21:107–37.
27. Ross GD, Vetvicka V. (1993) CR3 (CD11b, CD18): a phagocyte and NK cell membrane receptor with multiple ligand specificities and functions. *Clin. Exp. Immunol.* 92:181–4.
28. Darby I, Skalli O, Gabbiani G. (1990) Alpha-smooth muscle actin is transiently expressed by myofibroblasts during experimental wound healing. *Lab. Invest.* 63:21–9.
29. Hsu WC, Spilker MH, Yannas IV, Rubin PAD. (2000) Inhibition of conjunctival scarring and contraction by a porous collagen-glycosaminoglycan implant. *Invest. Ophthalmol. Vis. Sci.* 41:2404–11.
30. Reber F, Gersch U, Funk RW. (2003) Blockers of carbonic anhydrase can cause increase of retinal capillary diameter, decrease of extracellular and increase of intracellular pH in rat retinal organ culture. *Graefes Arch. Clin. Exp. Ophthalmol.* 241:140–8.
31. Scheuermann T, Sun Y, Sagner S, Rueger B. (2009) Gene expression analysis of paclitaxel-treated HT29 cells using the xCELLigence™ System and RealTime ready™ Panels. *Biotechniques.* 46:557–8.
32. Kim TH, et al. (2008) Co-treatment of suberoylanilide hydroxamic acid and mitomycin-C induces the apoptosis of rabbit tenon's capsule fibroblast and improves the outcome of glaucoma filtration surgery. *Curr. Eye Res.* 33:237–45.
33. Okada K, et al. (2009) Effects of mitomycin C on the expression of chymase and mast cells in the conjunctival scar of a monkey trabeculectomy model. *Mol. Vis.* 15:2029–36.
34. Mietz H, Arnold G, Kirchoff B, Diestelhorst M, Krieglstein GK. (1996) Histopathology of episcleral fibrosis after trabeculectomy with and without mitomycin C. *Graefes Arch. Clin. Exp. Ophthalmol.* 234:364–8.
35. Jampel HD. (1992) Effect of brief exposure to mitomycin C on viability and proliferation of cultured human Tenon's capsule fibroblasts. *Ophthalmol.* 99:1471–6.
36. Khaw PT, Sherwood MB, Mackay SLD, Rossi MJ, Schultz G. (1992) Five minute treatments with fluorouracil, floxudine, mitomycin have long-term effects on human Tenon's capsule fibroblasts. *Arch. Ophthalmol.* 110:1150–4.
37. Smith S, D'Amore PA, Dreyer EB. (1994) Comparative toxicity of mitomycin C and 5-fluorouracil in vitro. *Am. J. Ophthalmol.* 118:332–7.
38. Crowston JG, et al. (1998) Antimetabolite-induced apoptosis in Tenon's capsule fibroblasts. *Invest. Ophthalmol. Vis. Sci.* 39:449–54.
39. Khaw PT, et al. (1993) Prolonged localized tissue effects from 5-minute exposure to fluorouracil and mitomycin C. *Arch. Ophthalmol.* 111:263–7.
40. Francis BA, et al. (2005) Histopathologic features of conjunctival filtering blebs. *Arch. Ophthalmol.* 123:166–70.
41. Anand N, Arora S, Clowes M. (2006) Mitomycin C augmented glaucoma surgery: evolution of filtering bleb avascularity, transconjunctival oozeing, and leaks. *Br. J. Ophthalmol.* 92:175–80.